Journal of Nepal Geological Society, 2000, Vol. 22, pp. 179–186

Radiometric and geoelectric response of karst structures in Mahendra and Chamero Caves, Pokhara Valley, Nepal

Pitambar Gautam[1], Surendra Raj Pant[1], Hisao Ando[2], and Raghu Nath Wagle[1]
[1]*Central Department of Geology, Tribhuvan University, Kirtipur, Kathmandu, Nepal*
[2]*Suimonchishitsu Kenkyuusho (Institute of Hydrogeology Co. Ltd.), Sapporo 060-0004, Japan*

ABSTRACT

Natural gamma ray intensity and electrical resistivity measurements were made over the karst features (subsurface flow-channels, solution cavities, and sinkholes) forming the Mahendra and Chamero Caves in the Pokhara Valley, central Nepal. The layered basin-filling Quaternary clastic sediments comprising gravel, silt, and clay constitute the upper 60–80 m section of the Pokhara Valley. Depending mainly on lithology, they differ widely in electrical resistivity (a few hundreds to several tens of thousands of Ohm.m) making them suitable for mapping by resistivity methods. In favourable cases, electrical imaging is useful for assessing the layered structure as well as localised void spaces. Total gamma ray intensity profiles reveal significant anomalies (up to 100 counts per second) over the subsurface openings. The gamma-ray method is sensitive to near-surface cavities and is effective in locating the karstified structures, whereas the electrical images provide quantitative estimates of the depth to such features.

INTRODUCTION

A large volume of layered clastic deposits (gravel, silt and clay), of Quaternary age, has filled the Pokhara Valley (ca. 50 km x 5 km), which represents an intermontane fluvial basin spread around the midstream of the Seti River (Yamanaka et al. 1982). These deposits were brought from the Annapurna mountain range probably by a series of catastrophic debris flows. Because of the high amount of easily soluble calcareous material (25–65 %, by volume) in theses sediments, the Seti River and its tributaries have carved splendid river terraces and deep gorges. Karst structures (subsurface flow-channels, solution cavities, sinkholes, pinnacles, solution chimneys etc.) are widely developed both at the surface and underground. These karst structures, whether exposed or not, pose serious threat to houses, farmlands, and public work of any scale (e.g., the collapse of a highway bridge over the Seti River; Dhital and Giri 1993). Therefore, it is important to know the location in plan, and also the depth and lateral extent of such structures.

In this paper, we present some results of geophysical studies on buried karst structures undertaken within the Mahendra and Chamero Caves situated near Batulechaur. This cave system together with the Powerhouse area in the south and Gupteshwar-Patale Chhango Cave system in the southwest are the sites most affected by karstification and also the targets of our geophysical studies (Fig. 1). Our study was aimed at solving the following problems: (i) detection of the lateral and vertical changes in subsurface lithology on the basis of electrical resistivity (Keller and Frischknecht 1966); (ii) appraisal of the influence of the karstic features to the resistivity-depth models at relatively small scale (Ward 1990); and, (iii) delineation of shallow karst features by measuring the gamma ray counts (Nielson et al. 1990; Sharma 1997). The effectiveness of such approach in the areas located in the Powerhouse and Gupteshwar Cave areas has been already demonstrated (Gautam et al. 2000). Therefore, some new radiometric and electrical imaging data from the Mahendra and Chamero Caves will be given here.

GEOLOGY AND KARST STRUCTURES

The Quaternary deposits overlie the metasedimentary rocks of Precambrian age that form the basement of the Pokhara Valley. The deposits are divisible into 7 lithostratigraphic units: Begnas, Siswa, Tallakot, Ghachok, Phewa, Pokhara, and Rupakot Formations (Yamanaka et al. 1982). The Ghachok, Pokhara, and Phewa Formations are the major lithologies prone to the development of karstic features (Fig. 1). The Ghachok Formation is represented by extremely hard conglomerate bed made up of subangular to subrounded gravels of limestone, sandstone, and shale cemented by calcareous material. The Pokhara Formation is made up of fluvial gravels with intercalations of lacustrine sediments; the gravels comprise subangular to subrounded pebbles and cobbles of limestone and calcareous shale, which exhibit poor cementation, ill sorting, and partial stratification. The Phewa Formation comprises well stratified, porous, and comparatively weak deposits of calcarenite to calcisiltite composition.

A notable lithological unit is the gravel veneer on the fillstrath terraces carved in the Pokhara Terrace. The veneer gravels are of mainly cobble to boulder size, larger than those in the Pokhara Formation, mostly subrounded and scattered

in unsorted sandy matrix. The clasts are represented by mainly gneiss, granite, quartzite and schist. Major geomorphic units are: i) the Ghachok Terrace and Pokhara Terrace representing the accumulational fill-top landforms; ii) two groups of fillstrath terraces developed over the Ghachok and Pokhara Terraces, respectively, representing landforms formed by redeposition over eroded ancient terraces; and iii) recent flood plain (Yamanaka et al. 1982).

Speleological characteristics

The western part of the Pokhara Valley has at least 10 cave sites (Gebauer 1983), of which three prominent locations are indicated in Fig. 1. The Mahendra Cave system (M) comprising the Mahendra Cave and Chamero Cave is situated on the right bank of the Kali River. The Gupteshwar Cave system (G), which comprises the Patale Chhango (Devi's fall) and Gupteshwar Caves, occurs along the course of the Marde River. The Power Station Caves (P) are developed in the terrace scarps at the northern bank of the Phusre River. Gebauer (1983) noted that the Power Station Caves are developed in the caprock, composed of coarse conglomerate of relatively greater resistance to weathering, constituting the uppermost part of the river terrace. The Mahendra and Chamero Caves are developed below the coarse conglomerate of the caprock (which makes actually the ceilings of the caves). With a total length of 2959 m, the Patale Chhango (or

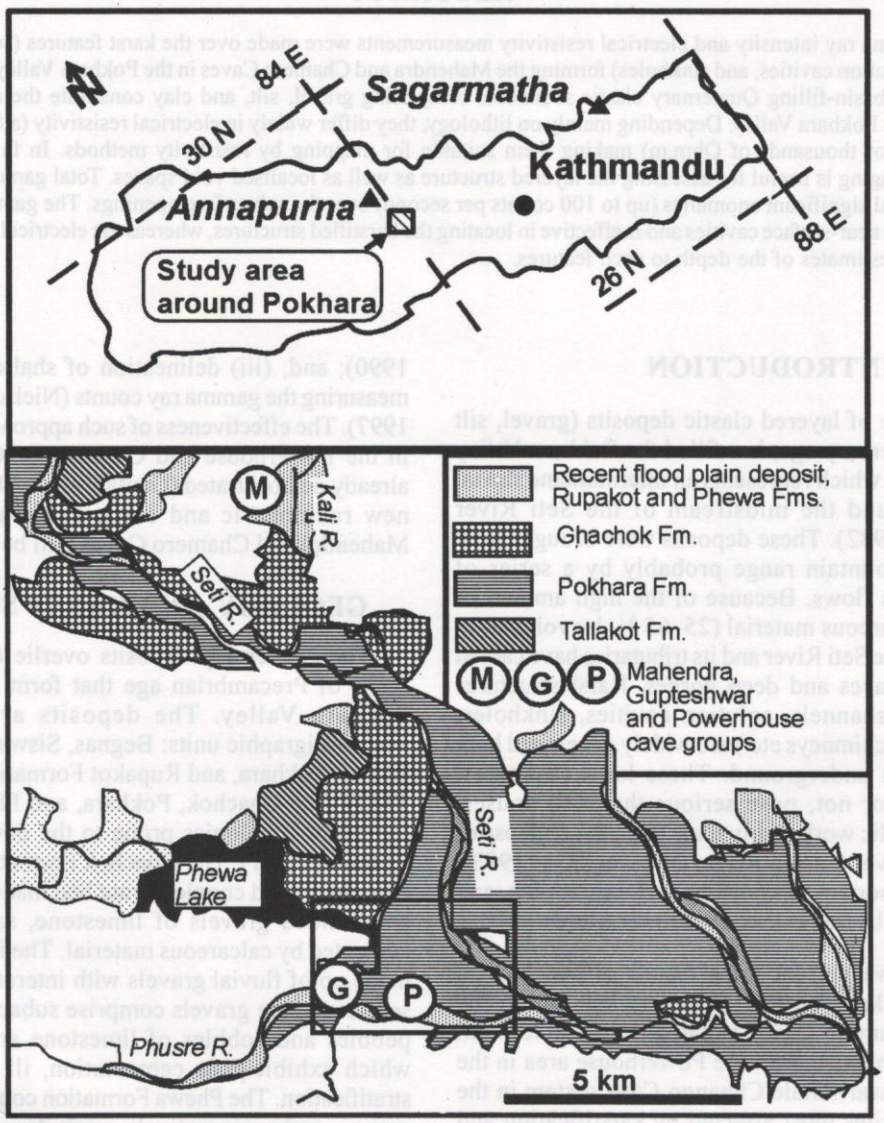

Fig. 1: Sketch map of Nepal showing the location of the Pokhara Valley (upper diagram) and schematic map of the study area (lower diagram) showing the major geologic formations (adapted from Yamanaka et al. 1982). Phewa Lake is shown in dark colour. Three prominent localities of the karstic features or caves (M, G and P) are shown after Gebauer (1983). Geophysical data obtained from the Mahendra Cave system are discussed here.

Devi's fall) Cave represents the longest cave in the Indian Subcontinent.

Koirala et al. (1996) noted that the Mahendra and Gupteshwar Caves, which are regularly visited by tourists and therefore represent the sites prone to hazard related to possible failures of certain parts, are developed within the Phewa Formation. In the Powerhouse area, subsurface flow channels or caves are developed within the conglomerate layers that constitute the upper part of the Pokhara Formation. These layers are actually overlain by a coarse gravelly conglomerate of the gravel veneers or caprocks. The floor of the caves consists of sediments represented by laminated fine sand, silt, and clay, which appear gray or light brown. The southern peripheries of the Powerhouse area, Gupteshwar Cave, and the Mahendra and Chamero Caves have high hazard of sinkhole development, subsidence, and also widespread pollution along the subsurface solution channels (Koirala et al. 1996).

GEOPHYSICAL INVESTIGATIONS

Research methodology

Field observations were made by employing two techniques: geoelectric imaging and radiometric profiling. Geoelectric imaging was done using a double-dipole array when two equi-dimensional current and electrode dipole pairs were spaced apart variously during successive measurements in several adjacent segments so as to obtain a continuous 2D (in vertical plane) coverage of the subsurface along selected profiles (Telford et al. 1976). A SAS 300-C Terrameter (ABEM, Sweden) was used for measurements. A GRS-500 portable differential gamma-ray spectrometer (Scintrex, Canada) equipped with 124 cc NaI(Tl) detector was used to measure the response mainly in T_{c1} energy window (total gamma-ray counts with gamma-ray energy Egg >0.08 MeV; recording period = 10 s).

RADIOMETRIC (GAMMA-RAY) PROFILES

Chamero Cave

This cave lies about five-minute walking distance to the NW of the Mahendra Cave situated at Batulechaur. It occurs behind a stone-walled and sparsely vegetated meadow, which is riddled with sinkholes of varying dimensions (Fig. 2; left diagram) The major karst features are: two large-scale collapses (I and II) shown in the schematic map, one karst doline, and two nearly circular sinkholes formed where the collapse No. I meets the karst doline. The main entrance to the cave lies at the bottom of the northern sinkhole. There exists a narrow opening, situated towards the SW of the main entrance, which may serve as an exit. Following the entrance, which occurs at 22 m depth at the base of a vertical wall to the NW corner of the northern sinkhole, one comes across two large galleries stretched roughly along N-S direction and connected by a low slit. The northern gallery is 18.6 m long, 12.5 m wide, and up to 6 m high. The southern gallery is 40 m long, 14.5 m wide and >6 m high. Though this cave also attracts a limited number of visitors and serves as a show cave, it is not electrically illuminated. Therefore, there are numerous bats (a bat is called *Chamero* in Nepali, hence the name of the cave) in the cave. The material constituting the cave wall is made up of silty matrix (60–70%) with abundant gravels. The clasts are predominantly angular to sub-rounded and their size rarely exceeds 12 cm. The overall amount of gravel decreases towards the cave floor. The material near the base is well cemented but it exhibits well-developed joints in different directions. Most of the minor depressions or sinkholes observed in the surface are of irregular shape with a depth of <1 m.

Gamma-ray measurements were made along several profiles (RC1–RC4; Fig. 2) of differing orientation. Results of profile RC2 (Fig. 2, upper right) show that there are significant variations in gamma-ray counts in all 4 modes of measurement but the most contrasting values are recorded at Tc1(soil) mode. For this reason, further measurements within the Mahendra-Chamero Cave system were made in Tc1(soil) mode and the data are presented simply as Tc1 counts. The elevated gamma-ray counts occur directly over the depressions of various scales caused by collapse/subsidence of the ground. This is better illustrated by profile RC3 (Fig. 2, lower right) that is accompanied by a topographical profile as well.

Mahendra Cave

This is an electrically illuminated show cave, which is easily accessible by the visitors. A sketch map of a part of the cave is given in Fig. 3 (left diagram). The main passage runs down from northwest to southeast with a trapezoid-shaped cross-section (5 m wide x 3 m high, in the average). After walking for about 40 m past the main entrance, one encounters a short side-passage slightly ascending across boulders and leading towards a narrow exit out of the cave. A comparison of the present sketch with the one made by Gebauer (1983), the former being prepared without the knowledge of the existence of the latter, reveals that this part of the cave has not changed much during the last 20 years.

Total count data recorded as Tc1(soil) for profiles RM1 and RM2 are presented in Fig. 3. A direct correlation between elevated readings and the localised void space or karstic features in the subsurface is evident.

ELECTRICAL IMAGING AND RESISTIVITY-DEPTH MODEL

Electrical imaging profiles were taken in both areas: profiles IM1 and IM2 in the Mahendra Cave area and profiles IC1, IC2, and IC4, which coincide with the radiometric profiles RC1, RC2, and RC4, respectively, in the Chamero Cave area (Fig. 2 and 3). However, owing to several unfavourable factors (e.g., uneven topography, difficulty to extend a given profile laterally owing to space limitations, extremely high

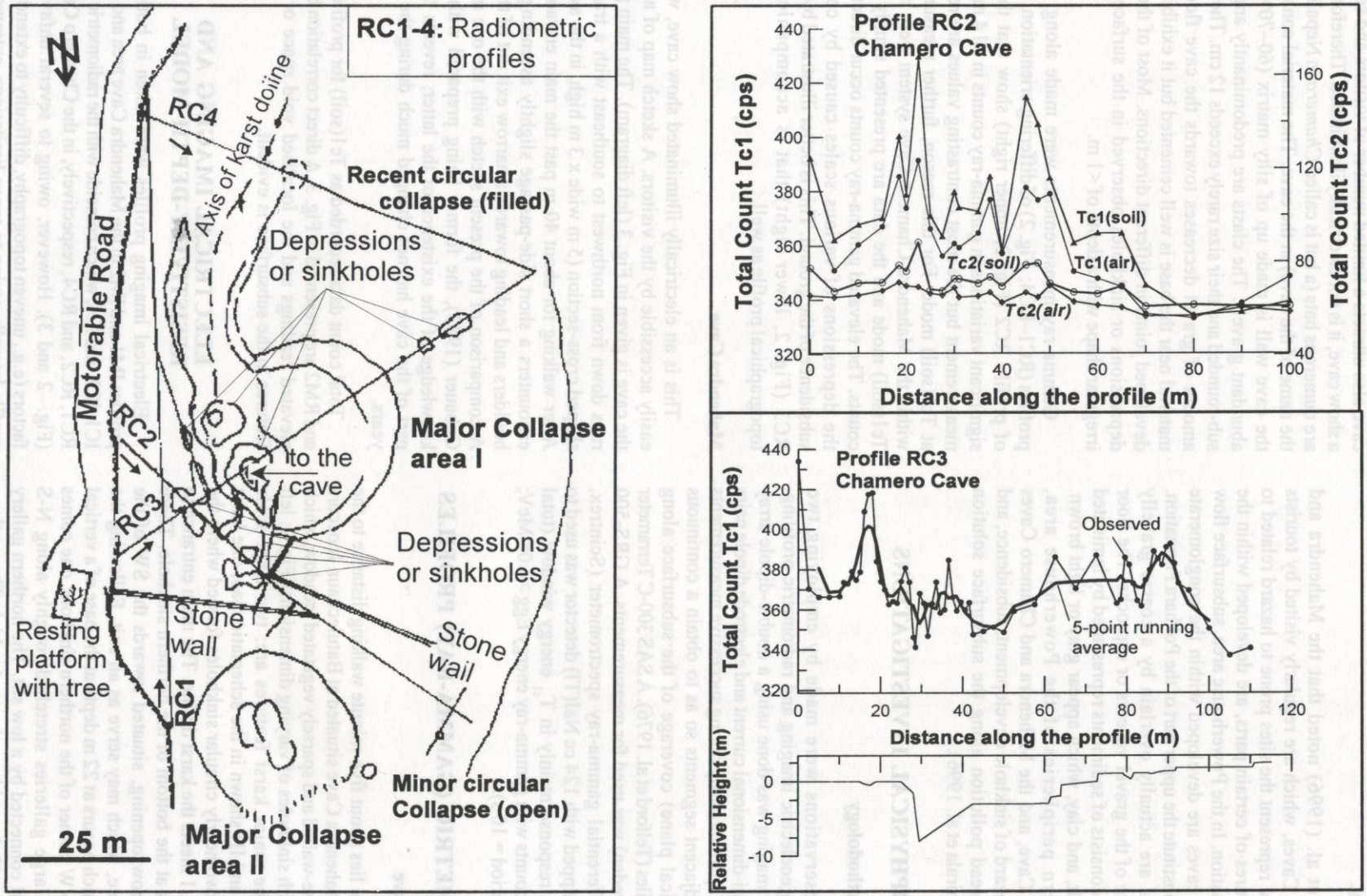

Fig. 2: Schematic sketch map of the Chamero Cave area and radiometric profile locations. Left: Surface karst features. Upper right: Comparison of the gamma-ray counts observed along profile RC2 in two total-count channels (Tc1 and Tc2) measured at the surface (soil) and waste height (air) modes. Lower right: Tc1 counts measured at the surface and the smoothed curve for profile RC3 together with an approximate topographic profile.

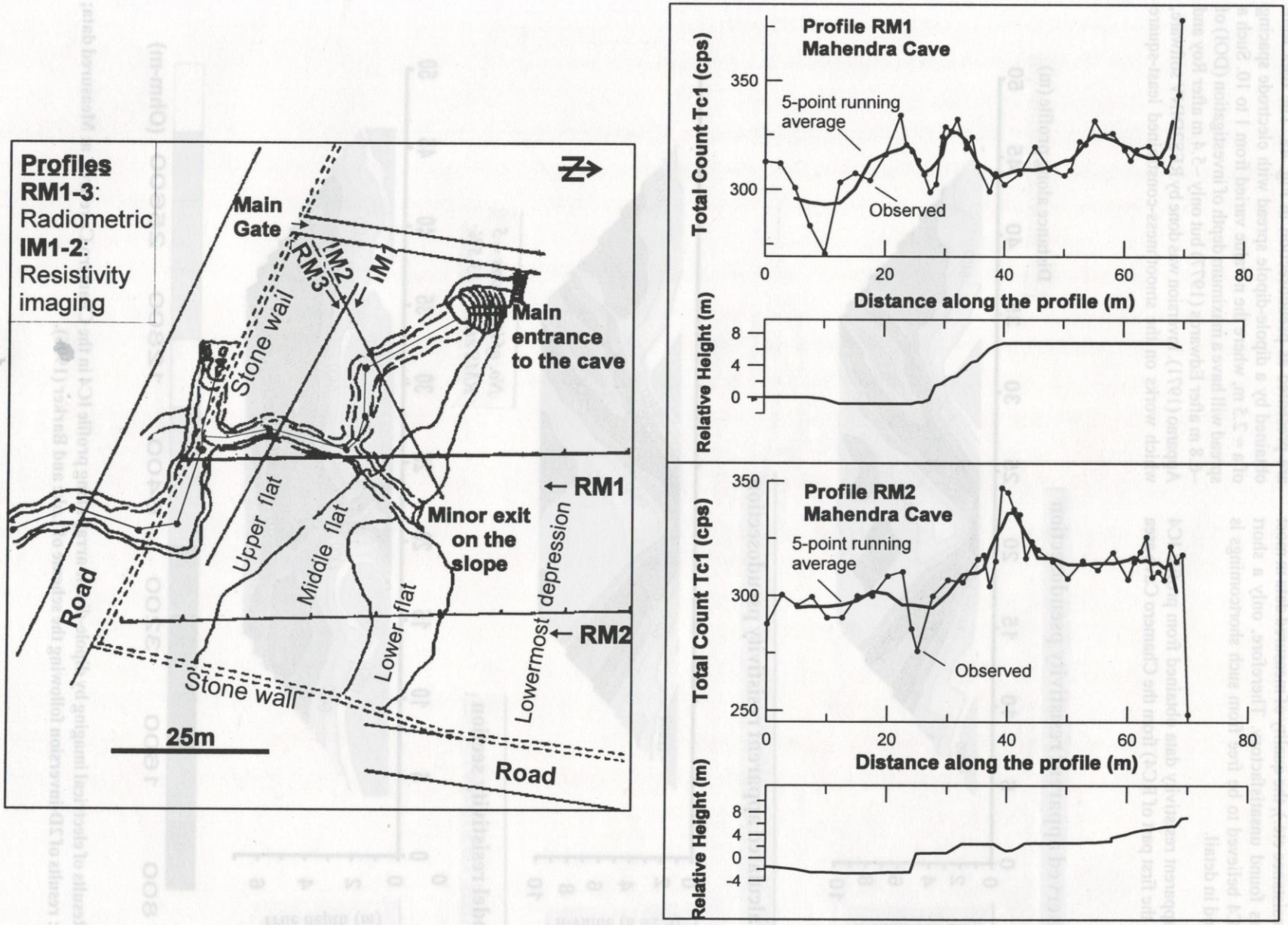

Fig. 3: Schematic sketch map of the Mahendra Cave area and profile locations. Left: Surficial karst features; Upper right: Tc1 counts measured at the surface and the smoothed curve for profile RM1; and Lower right: the same for profile RM2. Both diagrams are accompanied by approximate topographic profiles.

contact resistance etc.), the quality of measured data in most cases was found unsatisfactory. Therefore, only a short profile IC4 believed to be free from such shortcomings is considered in detail.

The apparent resistivity data obtained from profile IC4 (same as the first part of RC4) from the Chamero Cave area are presented as pseudosection in Fig. 4a. The data were obtained by a dipole-dipole spread with electrode spacing of a = 2.5 m, where the n-value varied from 1 to 10. Such a spread will have a maximum depth of investigation (DOI) of ~6.8 m after Edwards (1977) but only ~5.4 m after Roy and Apparao (1971). Inversion was done by RES2DINV software, which works on the smoothness-constrained least-square

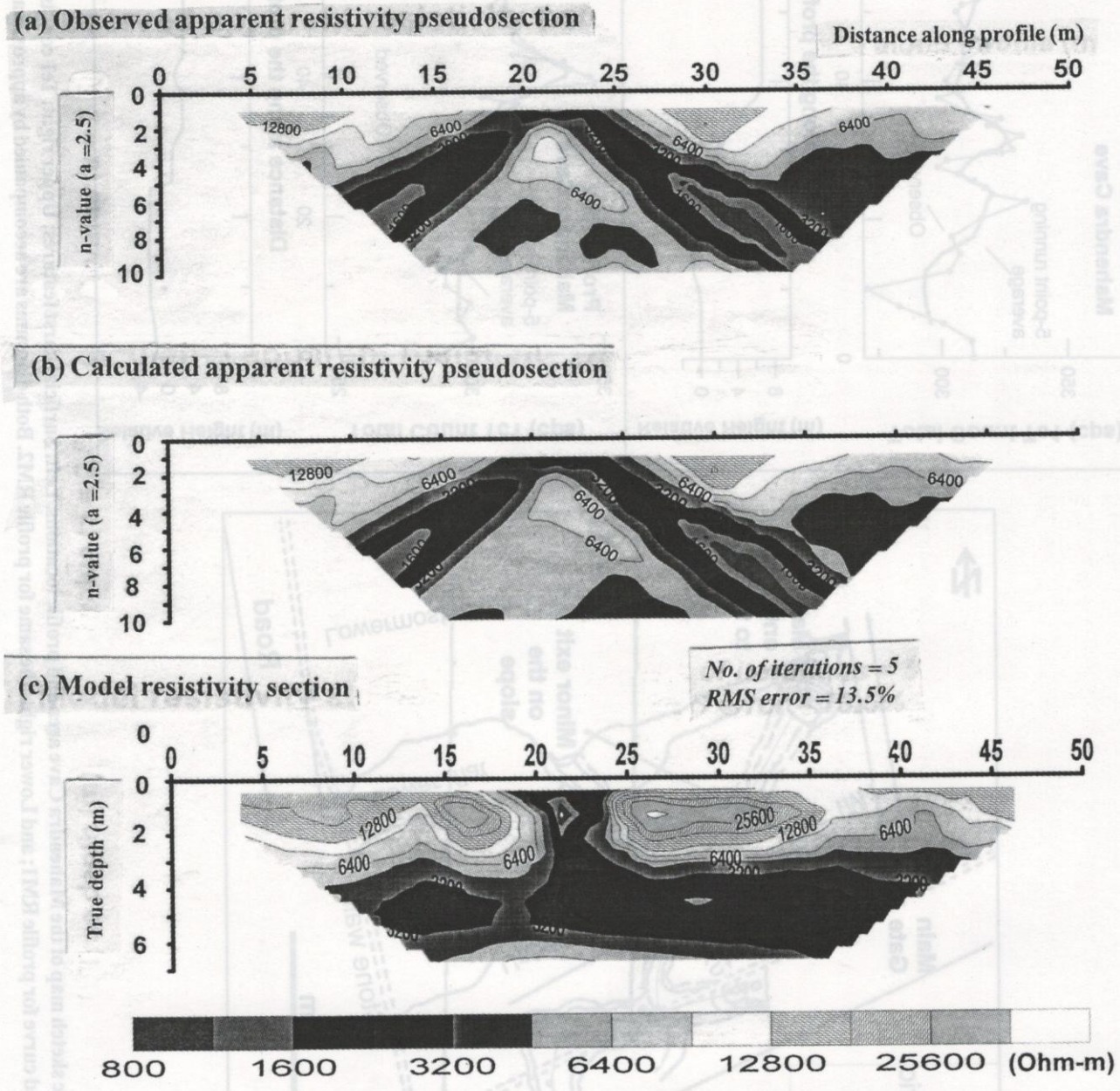

Fig. 4: Results of electrical imaging by dipole-dipole array along profile IC4 in the Chamero Cave area. a: Measured data; and b-c: results of 2D-inversion following the scheme of Loke and Barker (1996).

method with implementation of quasi-Newton optimization technique (Loke and Barker 1996). The resistivity-depth model consists of an arrangement of rectangular blocks loosely tied to the distribution of datum points in the pseudosection. The depth of the bottom row of blocks is set to be approximately equal to the DOI obtained after Edwards (1977).

Calculated apparent resistivity pseudosection and inverted model section for this profile are given in Fig. 4b and 4c. The model section suggests the presence of three layers. But only two upper layers, a very high resistivity layer on the top and an underlying low resistivity layer below it, are distinct. The localised sub-vertical zone with low-resistivity occurring in the upper layer probably represents a collapse zone, which was later filled up with soil from the surrounding area by local farmers.

CONCLUSIONS

The interpretation of gamma-ray counts in terms of subsurface lithology or mass distribution does not seem to be straightforward. This is because the measured gamma-ray activity in the field is a sum of contributions from radiations of differing origin: the background of the measuring instrument, intensity of cosmic rays, radioactivity of the constituent near-surface rock or soil medium, effect of possible radioactive fallout, and radon (primarily Rn^{222}) content in the air. The latter is known to fluctuate with the variations in temperature, humidity, and pressure, which affect the escape of radon from the rock or soil medium. With favourable circulation of radon and mineralised groundwater, the fracture and fault zones get enriched in the decay products of Ra and Rn and may be the sites of redistribution of K^{40}, U^{238}, and Th^{236}.

Though it is difficult to separate the differing contributions, it is known that the areas lying above the karst structures or fault/fracture zones show increased gamma activity due to the increased propagation of emission along the fissures or fractures to the surface (Surbeck and Medici 1990; Abdoh and Pilkington 1989; Sharma 1997). The direct correlation of the observed gamma-ray counts and the known subsurface karst features in the Mahendra and Chamero Caves suggests that this method is well suited for locating unknown features as well. The nature of such interpretation is largely qualitative due to the possible variations in the geometry of the subsurface karst features and the nature of the fractures occurring over such features. In addition, analysis of the close relationship between the magnitude of the radiometric anomaly and the dimensions of the buried karstic features will require the exact knowledge of the variation in topography of the area.

Electrical imaging may provide a better 2D-picture of the subsurface and allow the estimation of the depth of the features that have contrasting resistivity. However, this method will work only if the measured data are least influenced by topographical effects and other types of noise. Therefore, a geophysical complex involving radiometric mapping and electrical imaging profiles (e.g., with dipole-dipole array) is always better in assessing the depth, extent, and geometry of the buried subsurface karst features.

ACKNOWLEDGEMENTS

The authors appreciate the support and encouragement provided by Dr. P. C. Adhikary, Head of the Central Department of Geology, Tribhuvan University throughout this study. They are thankful to graduate students D. Bhattarai and J. Gurung for their participation in the field measurements. Funding for the fieldwork was provided through a collaborative programme between Japan International Cooperation Agency and the Central Department of Geology, Tribhuvan University.

REFERENCES

Abdoh, A. and Pilkington, M., 1989, Radon emanation studies of the Ile Bizard Fault, Montreal. Geoexploration, v. 25, pp. 341–354.

Dhital, M. R. and Giri, S., 1993, Engineering-geological investigations at collapsed the Seti Bridge site, Pokhara. Bull. Dept. Geol., Tribhuvan Univ., v. 3(1), pp. 119–141.

Edwards, L. S., 1977, A modified pseudosection for resistivity and IP. Geophysics, v. 42(5), pp. 1020–1036.

Gautam, P., Pant, S. R., and Ando, H., 2000. Mapping of subsurface karst structure with gamma ray and electrical resistivity profiles: a case study from Pokhara Valley, Central Nepal. Jour. Appl. Geophys., v. 45(2) pp. 97–110.

Gebauer, D. H., 1983, Caves of India and Nepal. Spelälogische Sud-Asien Expedition 1981/82, Germany. 166 p.

Keller, G. V. and Frischknecht, F. C., 1966, *Electrical Methods in Geophysical Prospecting*. Pergamon Press Inc. 519 p.

Koirala, A., Rimal, L. N., Sikrikar, S. M., and Pradhananga, U. B., 1996, Engineering and environmental geological map of Pokhara Valley. Published by Department of Mines and Geology (in cooperation with BGR, Germany), Lainchaur, Kathmandu, Nepal.

Loke, M. H. and Barker, R. D., 1996, Rapid least-squares inversion of apparent resistivity pseudosections by a quasi-Newton method. Geophysical Prospecting, v. 44, pp. 131–152.

Nielson, D. L., Linpei, C., and Wards, S. H., 1990, Gamma-ray spectrometry and radon emanometry in environmental geophysics. In: Ward, S.H. (Ed.) Geotechnical and Environmental Geophysics, Soc. Exp. Geophys., Tulsa, v. 1, pp. 219–251.

Roy, A. and Apparao, A., 1971, Depth of investigation in direct current methods. Geophysics, v. 36, pp. 943–959.

Surbeck, H. and Medici, F. , 1990, Rn-222 transport from soil to karst caves by percolating water. In: Proc. 22nd Congr. IAH, Aug. 27-Sept. 1, Lausanne.

Sharma, P. V., 1997, *Environmental and Engineering Geophysics*. Cambridge Univ. Press. 475 p.

Telford, W. M., Geldart, L. P., Sheriff, R. E., and Keys, D. A., 1976, *Applied Geophysics*. Cambridge University Press. 860 p.

Ward, S. H., 1990, Resistivity and induced polarization methods. In: Ward, S. H. (Ed.) Geotechnical and Environmental Geophysics, Soc. Exp. Geophys., Tulsa, v. 1, pp. 147–189.

Yamanaka, H., Yoshida, M., and Arita, K., 1982, Terrace landform and Quaternary deposits around Pokhara Valley, Central Nepal. Jour. Nepal Geol. Soc., v. 2, pp. 95–112.